Surface-Grafted Hyperbranched Polymers via Self-Condensing Atom Transfer Radical Polymerization from Silicon Surfaces

Hideharu Mori,[†] Alexander Böker,[†,‡] Georg Krausch,[‡,§] and Axel H. E. Müller*[,†,§]

Lehrstuhl für Makromolekulare Chemie II, Lehrstuhl für Physikalische Chemie II, and Bayreuther Zentrum für Kolloide und Grenzflächen, Universität Bayreuth, D-95440 Bayreuth, Germany

Received November 6, 2000

ABSTRACT: A novel synthetic concept for preparing hyperbranched polymers on a planar surface is described, in which a silicon wafer grafted with an initiator layer composed of an α-bromoester fragment is used for a self-condensing vinyl polymerization (SCVP) via atom transfer radical polymerization (ATRP). A large number of nanoscale protrusions were found on the surface obtained by (meth)acrylic AB* initiator-monomers ("inimers"). The variations of the size and density of the protrusions, as well as the film thickness, depend on the catalyst system and show a slight correlation with the degree of branching and molecular weight of the ungrafted polymers, as confirmed by scanning force microscopy (SFM). The surface roughness is much larger than that of polymer brushes obtained by polymerizing conventional (meth)-acrylates. The copolymerization of an AB* inimer and a conventional vinyl monomer gave an intermediate surface topography between the polymer protrusions and the polymer brush, which may be due to the highly branched structure. X-ray photoelectron spectroscopy (XPS) was used to determine the surface chemical composition. We find significant differences in the intensity of the bromine peak between the linear polymer brush, the branched, and the hyperbranched polymers, suggesting the feasibility of controlling the surface chemical functionalities.

Introduction

The manipulation and control of surface properties of thin polymer films have become progressively important in numerous commercially important technologies, such as biotechnology and advanced microelectronics. Surface grafting of polymer chains has been investigated as an effective and versatile method for this purpose.[1] Commonly, the grafted polymers were prepared by interaction of end-functionalized polymers or block copolymers with the surface.[2,3] These systems, however, have a limited grafting density as further grafting is hindered by the polymer chains already adsorbed on the surface. On the other hand, surface-initiated polymerization[4−6] has been employed for a variety of monomers in order to modify surfaces of solid substrates and to design the surface macromolecular architecture, such as polymer brushes. To obtain well-defined polymer brushes, several requirements have to be met including controlled surface grafting density and monodisperse polymer chains, which might be achieved with living polymerization methods. Such brushes consist of end-grafted, strictly linear chains of the same length, and the chains are forced to stretch away from the interface. A high grafting density and a brush height significantly larger than the unperturbed radius of gyration can be obtained. The well-defined brushes can be used further to prepare smart materials to serve as functional devices on a nanometer scale, since they react collectively to environmental stimuli such as changes of the pH or ionic strength, temperature, solvent quality, or mechanical forces.[7] Hence, several attempts have been conducted to accomplish controlled/"living" polymerizations on a surface utilizing cationic,[8,9] anionic,[10,11] radical,[12−17] and ring-opening[18−20] methods.

Highly branched polymers are of considerable scientific and industrial interest, due to their low intrinsic viscosity, high solubility, and miscibility and their potential as polyfunctional carriers. In recent years, there have been several studies of dendrimers grafted to surfaces.[21] Due to the highly compact and globular shape, as well as the monodispersity, they are useful for many potential applications, such as data storage or nanolithography systems. Recently, Zhou et al.[22] reported the preparation of a highly branched poly(acrylic acid) film attached to a self-assembled monolayer of mercaptoundecanoic acid on gold using a series of repeated "grafting to" steps. The advantage of the system is that each new layer contains more polymer branches than the previous one, and thus is more tightly packed. They demonstrated that the hyperbranched polymers can be covalently modified with a broad range of functional groups, such as fluorophores, electroactive groups, perfluorinated moieties, dyes, and even other polymers. The surface-confined hyperbranched polymers are suitable for a number of technical applications, including corrosion inhibition, chemical sensing, cellular engineering, and micrometer-scale patterning.[23] However, both approaches have the disadvantage that many tedious synthetic steps are necessary to reach the defined surface structures.

Several strategies for the preparation of hyperbranched polymers are currently employed, the most common method being the polycondensation of AB_n monomers. The recent discovery of self-condensing vinyl polymerization (SCVP) by Fréchet et al.[24] made it possible to use vinyl monomers for the one-step synthesis of hyperbranched structures. This reaction is based on an initiator-monomer ("inimer") of the general structure AB*, where the double bond is designated A and B* is a group capable of initiating the polymerization of vinyl groups. Living cationic and radical polymerizations, group transfer polymerization, and ring-

[†] Lehrstuhl für Makromolekulare Chemie II.
[‡] Lehrstuhl für Physikalische Chemie II.
[§] Bayreuther Zentrum für Kolloide und Grenzflächen.
* Corresponding author. e-mail: Axel.Mueller@uni-bayreuth.de.

10.1021/ma0019048 CCC: $20.00
Published on Web 08/18/2001

opening polymerization have been applied to SCVP.[25−33] Since the disclosure of the above reaction, it has also been shown that the copolymerization of AB* inimers with conventional monomers yields macromolecules with branched structures, allowing to control molecular weight and molecular weight distribution.[26,34,35] The copolymerization method is a facile approach to obtain functional branched polymers, because different types of functional groups can be incorporated into a polymer depending on the chemical nature of the comonomer. In addition, the chain architecture can be modified easily by a suitable choice of the comonomer ratio in the feed.

In this paper we describe a novel synthetic approach to prepare hyperbranched polymers grafted from a planar surface. A silicon wafer grafted with an initiator, B*, for controlled/"living" radical polymerization is used for SCVP, as illustrated in Scheme 1. Because both the AB* inimer and the functionalized silicon wafer have groups capable of initiating the polymerization of vinyl groups, the chain growth can be started from both B* in the initiators immobilized on the silicon wafer and a B* group in the inimer. Both of the activated B* can add to the double bond, A, to form the ungrafted or grafted dimer with a new propagating center, A*. Further addition of AB* inimer or dimer to A* and B* centers results in hyperbranched polymers. Because the polymer formed in solution may also add to active centers of attached polymers, the method described here can be considered as a combination of "grafting from" and "grafting to" approaches. Atom transfer radical polymerization (ATRP) was used in this study, because of (a) the feasibility of attaining controlled polymerization of conventional monomers from a surface,[12−17] (b) the significant influence of various factors on the degree of branching, molecular weight and polydispersity of a branched polymer obtained by SCVP[29] (the ratio of Cu(I)/Cu(II), the ligand used to complex copper, solvent, and temperature), (c) compatibility with a wide variety of monomers (e.g., acrylates, styrenes, acrylonitrile, and derivatives), and (d) easy handling compared to other living systems. The one-step self-condensing ATRP from the surface can be regarded as a novel and convenient approach toward the preparation of smart interfaces. The thin polymer films obtained may have a high density of functional groups at the interface and a characteristic surface topography due to the hyperbranched architecture. In this study, we discuss the surface morphology of the polymer films grafted from the surface as a function of the structure of AB* inimer and the ratio $[AB^*]_0$:$[\text{catalyst}]_0$. The surface topography and composition of the surface-grafted polymer layers were investigated by scanning force microscopy (SFM) and X-ray photoelectron spectroscopy (XPS).

Scheme 1

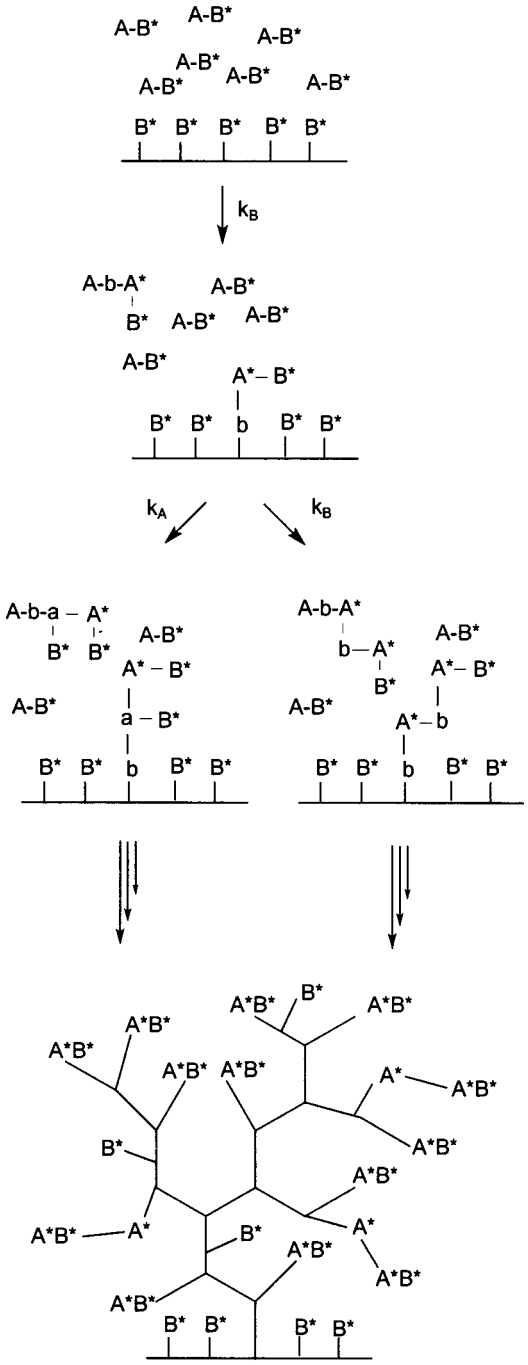

Experimental Section

Materials and Momomers. CuBr (95%, Aldrich) was purified by stirring overnight in acetic acid. After filtration, it was washed with ethanol, ether, and then dried. *N*,*N*,*N*′,*N*″,*N*″-Pentamethyldiethylenetriamine (PMDETA, 99%, Aldrich) and ethyl 2-bromo-2-isobutyrate (EBIB, 98%, Aldrich) were distilled and degassed. Bis(triphenylphosphine)nickel(II) bromide ($(PPh_3)_2NiBr_2$, 99%, Aldrich) was used as received. *tert*-Butyl acrylate (tBuA, BASF AG) was fractionated from CaH_2, stirred over CaH_2, and distilled and degassed in high vacuum. Methyl methacrylate (MMA, Röhm GmbH) was stirred over CaH_2 and then distilled and degassed. Other reagents were commercially obtained from Aldrich and used without further purification. Syntheses of (meth)acrylic AB* inimers, 2-(2-bromopropionyloxy)ethyl acrylate (BPEA) and 2-(2-bromoisobutyryloxy)ethyl methacrylate (BIEM), were conducted by the reaction of an α-bromoacid halide with 2-hydroxyethyl (meth)acrylate in the presence of pyridine as reported previously.[27] These inimers were degassed by three freeze−thaw cycles.

Synthesis of α-Bromoester Type Initiator on Silicon Wafer. The preparation of the α-bromoester initiator attached to a silicon wafer was conducted by reaction of the crude trichlorosilyl derivative with a silicon wafer in a manner similar to that reported previously by Husseman et al.[13] The trichlorosilyl α-bromoester, which has reactive species capable of bonding to the surface and a latent α-bromoester, was prepared by the reaction of hex-5-enol with 2-bromo-isobutyryl bromide, followed by the hydrosilylation reaction with trichlorosilane. Silicon (100) wafers, cut into 1.2 × 1.6 cm^2 pieces, were cleaned in absolute ethanol, acetone, and toluene baths

Table 1. Polymerization Conditions of AB* Inimers with the Functionalized Silicon Wafer and Properties of Soluble Polymers

entry	AB*	$[AB^*]_0$:$[catalyst]_0$	temp (°C)	time (h)	x^a (%)	$M_n{}^b$	$M_w/M_n{}^b$	b^c	r^d	DB^e
1[f]	BPEA	50	30	0.25	97	4600	2.32	0.44	3.8	0.49
2[f]	BPEA	125	30	2	95	4200	2.28	0.38	5.8	0.47
3[f]	BPEA	200	30	24	89	3300	2.49	0.29	11.5	0.43
4[f]	BPEA	100	50	0.25	89	4100	2.21	0.21	26.2	0.36
5[g]	BPEA	100	50	3	8					
6[g]	BPEA	100	100	2	gel					
7[g]	BIEM	50	100	2	79	4300	2.83			
8[g]	BIEM	125	100	2	65	4400	3.82			

[a] Conversion of the double bonds as determined by ^{1}H NMR. [b] As determined by GPC vs linear polystyrene standards, after column purification of ungrafted polymers. [c] Fraction of reacted B* units as determined by ^{1}H NMR. [d] $r = k_A/k_B$, as determined according to eq 1. [e] Degree of branching as determined according to ref 36. [f] Bulk polymerization with CuBr/*N*,*N*,*N*′,*N*″,*N*″-pentamethyldiethylenetriamine (PMDETA). [g] Bulk polymerization with $(PPh_3)_2NiBr_2$.

under ultrasonic treatment for 5 min and dried in a nitrogen stream. The sample was oxidized with a mixture of concentrated H_2SO_4 and 30% H_2O_2 (50/50 vol %) at room temperature overnight. The wafers were rinsed with ultrapure hot H_2O (80−90 °C), cleaned in an ultrapure H_2O bath at room temperature under ultrasonic treatment for 3 min, and allowed to stand in fresh ultrapure H_2O at 80−90 °C for 15 min. The samples were removed from the bath and finally cleaned in a stream of CO_2 crystals ("snow jet"). Freshly cleaned silicon wafers were placed into a dried flask, followed by dry toluene (5 mL) and the crude trichlorosilyl derivative (1 mL, ca. 0.6 mmol). Then triethylamine (1 mL, 7.2 mmol) was added dropwise to the mixture under nitrogen, and the reaction mixture was allowed to stand for 18 h at room temperature without stirring. The wafer was then removed from the solution, rinsed repeatedly with methanol followed by dichloromethane, and then left to stand in dichloromethane for 18 h. The procedure was then repeated, and finally the wafers were dried in a nitrogen stream to give functionalized silicon surfaces, which were used immediately for the polymerization or stored at room temperature in a drybox. The mean roughness of the functionalized silicon wafer determined by SFM was about 0.6 nm in a 3 × 3 μm^2 region.

Polymerization. CuBr/PMDETA and bis(triphenylphosphine)nickel(II) bromide ($(PPh_3)_2NiBr_2$) were used as catalyst systems for the polymerization of acrylic and methacrylic monomers/inimers, respectively. All polymerizations were carried out in a round-bottom flask sealed with a plastic cap. A representative example is as follows: Distilled and degassed BPEA (1.92 g, 7.65 mmol) was added to a round-bottom flask containing the functionalized silicon wafer and CuBr(I) (0.0220 g, 0.153 mmol). As soon as PMDETA (0.0266 g, 0.153 mmol) was added, the system became green, indicating the start of the polymerization. The covered flask was allowed to stand at 30 °C, and the characteristic green color kept constant during the polymerization. Since the reaction was performed in bulk, the content of the flask was completely solidified when conversion reached a certain level. After 15 min, the polymerization was stopped by cooling. Conversion of the double bonds detected by ^{1}H NMR of the ungrafted material was 97%. After the mixture was dissolved in THF and was subsequently passed through a neutral alumina column, GPC measurement was conducted. The soluble polymer had a M_n = 4600 and a M_w/M_n = 2.32 (as determined by GPC using linear polystyrene standards). The wafer was removed from the mixture and rinsed with THF. Afterward, any absorbed polymer formed was removed from the wafer by Soxhlet extraction in THF for 24 h. Upon removal from the extractor, the wafer was dried under nitrogen and stored at room temperature in air. The determination of the proportion of B* in the ungrafted polymers was performed by evaluation of ^{1}H NMR spectra according to a method reported previously.[27] The proportions of b and B* could be calculated: b = (signal at 1.0−1.3 ppm which is formed by activation of the B* and subsequent addition of monomer)/(sum of signals at 1.0−1.3 ppm and signals at 1.75 ppm, the latter assigned to CH_3 of the 2-bromopropionyloxy group, B*); $B^* = 1 - b$. The reactivity ratio of A* and B* groups, $r = k_A/k_B$, was determined from eq 1.[28]

$$r = k_A/k_B = (x + B^* - 1)/[-\ln(B^*) + B^* - 1] \qquad (1)$$

where B^* is the proportion of B* groups in the soluble polymer and x is the conversion of double bonds. The degree of branching (DB) was determined as reported previously.[36] Under the condition described above, b = 0.44 was observed, corresponding to $r = k_A/k_B$ = 3.8 and DB = 0.49. For a polymerization of BIEM, a mixture of BIEM (0.906 g, 3.25 mmol) and $(PPh_3)_2NiBr_2$ (0.0483 g, 0.065 mmol) was heated at 100 °C for 2 h. Conversion of the double bonds detected by ^{1}H NMR of the ungrafted material was 79%, with a M_n = 4300 and a M_w/M_n = 2.83 (as determined by GPC using linear polystyrene standards). In some cases (for example, entries 1, 4, and 7 in Table 1), the residual polymer was again dissolved in a small amount of THF and poured into methanol (or methanol/water) to precipitate the polymer, which was used to determine the molecular weight by ^{1}H NMR, assuming one double bond per macromolecule.

Similarly, the copolymerization of a (meth)acrylic AB* inimer with a conventional monomer (tBuA or MMA) was carried out in the presence of the functionalized silicon wafer. In a typical experiment, BPEA (0.371 g, 1.48 mmol) was added to a round-bottom flask containing the functionalized silicon wafer, CuBr(I) (0.0207 g, 0.144 mmol), PMDETA (0.0253 g, 0.146 mmol), and tBuA (1.86 g, 14.5 mmol). The flask was placed in an oil bath at 60 °C for 5 h. Conversion was >98%, with a M_n = 7500 and a M_w/M_n = 3.32 (as determined by GPC using linear PtBuA standards). The PtBuA and PMMA brushes were also prepared by surface-initiated ATRP with ethyl 2-bromo-2-isobutyrate (EBIB) as an added or controlling initiator. A typical experiment for homopolymerization is as follows: EBIB (0.0360 g, 0.185 mmol) was added to a round-bottom flask containing the functionalized silicon wafer, CuBr(I) (0.0265 g, 0.185 mmol), PMDETA (0.0332 g, 0.192 mmol), and tBuA (2.96 g, 23.1 mmol). The mixture was heated at 60 °C for 15 h. Conversion was 97%, with a M_n = 15 800 and a M_w/M_n = 1.21 (as determined by GPC using linear PtBuA standards). The ungrafted polymers obtained by the homo- and copolymerizations were removed in a manner similar to that obtained by SCVP of AB* inimers.

Characterization. After preparation, the polymers bound only loosely to the surface were washed with THF and subsequently passed through a neutral alumina column to remove the catalyst residues. The remaining solution was characterized by GPC using THF as eluent at a flow rate of 1.0 mL/min at room temperature. Column set: 5 μm PSS SDV gel, 10^2, 10^3, 10^4, 10^5 Å, 30 cm each; detectors: Waters 410 differential refractometer and Waters photodiode array detector operated at 254 nm. Narrow PS standards (PSS, Mainz) were used for the calibration of the column set. The calibration curves of PtBuA and PMMA were used for the polymers obtained by homo- and copolymerizations of tBuA or MMA, respectively. ^{1}H NMR spectra were recorded in $CDCl_3$ with a Bruker AC-250.

Scanning force microscopy (SFM) images were taken on a Digital Instruments Dimension 3100 microscope operated in Tapping Mode (free amplitude of the cantilever ≈ 30 nm, set point ratio ≈ 0.98). Film thicknesses were observed by applying a scratch to the polymer film and subsequent SFM topography imaging in the vicinity of the scratch.[37] The values reported were determined as averages over an array of cross sections (>25 sections) of at least four different areas (two independent scans at different places) in SFM. Care was taken to remove the polymer within the scratch without damaging the substrate surface. Experimental uncertainties are approximately ±10% in the thickness as determined by the statistical error of thickness measurement at different areas. The diameter and density of the protrusions obtained by SCVP were determined by means of the particle analysis tool in the Nanoscope III software on the basis of a threshold height of about 5.0 nm in all cases. This procedure systematically underestimates the lateral extension of the particles, due to the well-known broadening of surface features by convolution with the finite size of the AFM tip. We assume that all tips had a tip radius of 10 nm. This value was subtracted from the measured diameter of the protrusions. The thickness of several samples was also confirmed by ellipsometery operating with a 633 nm He/Ne laser at a 70° incident angle. The following refractive indices were used for the various layers: 3.8816 for native silicon, 1.462 for silicon oxide, 1.460 for initiator layer, and 1.466 for poly(BPEA) (value from poly(*n*-butyl acrylate)). The surface coverage, Γ (mg/m^2), and grafting density, Σ (chains/nm^2), of polymer films were calculated by the following equations:[2]

$$\Gamma = h\rho \tag{2}$$

$$\Sigma = \Gamma \times 10^{-21} N_A / M_n \tag{3}$$

where h is the thickness of the layer, $\rho = 1.1$ g/cm^3 is the mass density of PMMA, N_A is Avogadro's number, and M_n is the number-average molecular weight.

X-ray photoelectron spectroscopy (XPS, Leybold) with a monochromatic Mg Kα X-ray source ($E_{exc} = 1256.3$ eV) and a hemispherical analyzer was used to characterize the surface chemical composition of the functionalized silicon wafer and the surface-grafted polymers. The base pressure during acquisition of the XPS spectra was approximately 5.0×10^{-8} mbar, and the spot size was 2×7 mm^2. All binding energies (BEs) were referenced by setting the CH_x peak maximum in the C_{1s} spectrum to 285.0 eV. Survey scans (0−1200 eV) were acquired at one location on the sample at an analyzer pass energy of 200 eV. All spectra were recorded at a takeoff angle of 90°, which is defined as the angle between the horizontal axis of the surface and the axis of the analyzer lens system.

Results and Discussion

Characterization of the α-Bromoester Initiator on Silicon Wafer. In this study, the α-bromoester group was selected as a group capable of initiating from both the surface and the AB* inimer. The formation of densely covered monolayers of a 2-bromoisobutyryl fragment on a silicon wafer was conducted by reaction of the crude trichlorosilyl compound with a silicon wafer. Subsequently, the sample was washed in methanol and dichloromethane repeatedly in order to remove free attachable initiator from the monolayer. Characterization of the functionalized silicon surface was carried out by XPS. Figure 1 displays a typical XPS survey spectrum of the functionalized silicon wafer. The C_{1s} (285 eV) and O_{1s} (533 eV) peaks associated with the organic portion of the attachable initiator along with a small Br_{3d} signal (70 eV) are seen in the spectrum. The observed atomic composition of oxygen is significantly higher than the expected value based on the chemical structure of the initiator, indicating that the detected

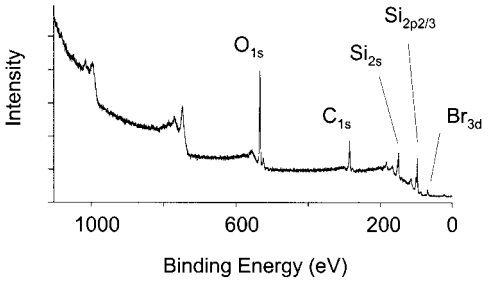

Figure 1. XPS survey spectrum of the functionalized silicon wafer.

O_{1s} peak is due to both the organic layer and SiO_x. The Si_{2s} and $Si_{2p3/2}$ peaks are also observed at 150 and 98 eV, respectively. This indicates that the thickness of the organic layer is smaller than the escape depth of the photoelectrons, suggesting that a very thin layer of the initiator forms on the silicon surface.

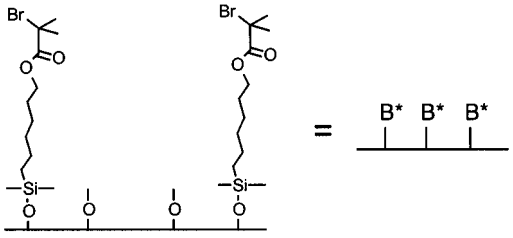

It has been reported that bromo-terminated monolayers are susceptible to damage by X-rays and secondary electrons during XPS.[38,39] Therefore, the Br peak intensity was monitored as a function of exposure time. The initial intensity of the Br_{3d} peak decreased with time (less than 30% was found after 6.5 h exposure). To correct for this effect, the C_{1s} to Br_{3d} ratio was determined as a function of X-ray dose, and the zero dose value was determined by extrapolation. The relative atomic composition obtained from the corrected Br peak area was approximately 11% Br and 89% C, which are (within the experimental error of about 10%) in agreement with the structure of the initiator molecule grafted on the surface (9% Br and 91% C). These XPS measurements of the functionalized silicon wafer consistently indicate the formation of the initiator layer on the surface and absence of other chemical functionalities.

SCVP from the Functionalized Silicon Wafer. For the preparation of hyperbranched polymers, BPEA (**1**) and BIEM (**2**) were used as acrylic and methacrylic AB* inimers, respectively. Hyperbranched polymers were synthesized by SCVP of the (meth)acrylic AB* inimers with the functionalized silicon wafer. Although a variety of catalyst systems and polymerization conditions are applicable, a suitable choice is required to fulfill the advantages of surface-initiated SCVP for the preparation of hyperbranched polymers grafted to the surface. Attempts to attain polymers quantitatively having a high degree of branching and a high grafting density were made by adjusting the catalyst system and polymerization conditions.

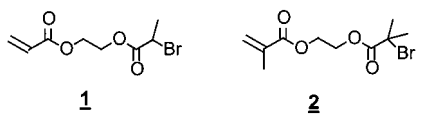

1 **2**

Polymerization of the acrylic AB* inimer, BPEA, with the functionalized silicon wafer was carried out in the presence of CuBr and PMDETA. The results are shown in Table 1. Because chain growth can be started from both the B* initiators immobilized on the silicon wafer and from B* groups in the inimers (Scheme 1), both ungrafted and grafted polymers can be produced. The unattached polymer chains were separated from the covalently bound polymers by washing with an appropriate solvent (THF) and used to estimate the molecular weight, the molecular weight distribution, and the degree of branching. When the reaction was performed at a ratio $[BPEA]_0:[CuBr]_0 = 50$, after 15 min at 30 °C, a viscous polymer with apparent number-average molecular weight $M_n = 4600$ and polydispersity index $M_w/M_n = 2.32$ (as determined by GPC using linear polystyrene standards) was obtained. In living polymerizations of conventional monomers from surface-grafted initiators, the molecular weight distribution of the grafted polymers is often assumed to be almost equal to that of polymer initiated by added soluble initiators.[13,14] Unfortunately, this is not the case for SCVP. The calculated molecular weight distribution of polymers formed in SCVP without initiators (conventional SCVP in solution) is broader than that obtained from SCVP in the presence of f-functional initiators.[40−42] Thus, the molecular weight and molecular weight distribution obtained here are only estimates. However, they may be used as relative values in order to compare polymers obtained under different conditions. The proportion of B* units in the soluble polymer, which can be observed by evaluation of ^{1}H NMR spectra, corresponded to a reactivity ratio, $r = k_A/k_B = 3.8$, indicating that addition of monomer occurred at A* centers at a rate approximately 4 times faster than that at B* centers. From this value, a degree of branching DB = 0.49 can be calculated.[36] For the batch conditions used here (inimers and initiators grafted on the surface are mixed spontaneously), the effect of the f-functional initiators on the degree of branching was calculated to be negligible.[40] This means that the degree of branching does not depend on whether polymer is formed in solution or on a surface. Hence, the result obtained here suggests the formation of highly branched polymers by SCVP of BPEA.

The degree of branching and molecular weight decreased with increasing $[BPEA]_0:[CuBr]_0$ ratio, while the ratio had only a slight effect on the polydispersity of the soluble polymer (Table 1, entries 1−3). Note that the calculated reactivity ratio in conventional SCVP in solution was $r = 4.5$,[28] which was explained on the basis of the dynamics of the activation equilibrium. An increase in polymerization temperature led to a decrease in the degree of branching. SCVP of BPEA with $(PPh_3)_2NiBr_2$, which was mainly employed for the methacrylic type monomers as described later, provided a polymer gel or only a small amount of polymer (Table 1, entries 5 and 6), suggesting that the Ni-based catalyst is not suitable for SCVP of the acrylic AB* inimer.

SCVP of the methacrylic AB* inimer, BIEM, was also conducted with the functionalized silicon wafer in the presence of $(PPh_3)_2NiBr_2$ at 100 °C. No significant difference was observed in the apparent molecular weights of soluble polymers obtained from BPEA and BIEM under the same $[AB^*]_0:[catalyst]_0$ ratio, as shown in Table 1. The relatively low apparent molecular weight of the resulting polymers may be due to the hyperbranched structure, as branched polymers have smaller hydrodynamic volumes than their linear analogues. The molecular weight determined by ^{1}H NMR, assuming one double bond per macromolecule, was 1.5−3 times higher than that determined by GPC. The difference in the molecular weights also supports the highly branched structure. The polydispersities of soluble polymers obtained from BIEM were slightly higher than those obtained from BPEA.

Table 2. Parameters of the Grafted Polymers Obtained from AB* Inimers

sample[a]	mean film thickness[b] (nm)	mean roughness[b] (nm)	areal density of protrusions[c] (μm^{-2})	surf. coverage[d] (mg/m^2)
1	4.0	2.2	67	4.4
2	7.5	3.1	57	8.3
3	11.0	3.6	42	12.1
7	4.5	1.5	94	5.0
8	12.0	2.0	47	13.2

[a] See Table 1. [b] As determined by SFM. [c] Density of protrusions was calculated on the basis of the threshold height of about 5 nm. [d] Surface coverage = film thickness × density (1.1 g/cm^3 for PMMA).

Unfortunately, we were not able to determine the molecular weight, polydispersity, and degree of branching of the grafted polymers by cleaving them from the surface, because the amount of polymer grafted onto the surface is extremely small (microgram range). Experiments aiming to determine the structural characteristics of the surface-grafted hyperbranched polymers obtained by this method are currently under way and will be reported elsewhere.

Surface Topography. Tapping mode SFM was used to investigate the surface topography of the grafted hyperbranched polymers after Soxhlet extraction in THF for 24 h. At least three scans at different spots on the sample were taken. Table 2 presents various parameters of the surface-grafted polymers obtained from SCVP of AB* inimers. Figure 2 shows a typical topography image of the polymer obtained from SCVP of BPEA at a ratio $[BPEA]_0:[CuBr]_0 = 125$. Protrusions are clearly visible on all height images. The protrusions were not detected on the functionalized silicon wafer prior to polymerization. The mean film thickness of the polymer layer determined by SFM topography imaging in the vicinity of the scratch was 7.5 ± 1.0 nm. The film thickness obtained by ellipsometry was 7.0 ± 1.0 nm in this case. Prolonged Soxhlet extraction had no effect on the film thickness and surface topography, indicating that the remaining polymer is covalently linked to the silicon wafer and any loosely bound polymer chains are completely removed by the treatment.[43] Parts b and c of Figure 2 represent a magnification of one representative protrusion and the cross section of the dotted line in the magnification, respectively. These images indicate that a typical protrusion corresponds to a broad dome structure having a height of about 10 nm. The mean diameter of the protrusions determined by SFM on the basis of the threshold height of 5.0 nm after subtracting the tip radius is about 30 nm. When a linear polymer brush is prepared by the "grafting-to" approach, the film thickness is limited to about $2R_g$ (the radius of gyration of a random coil polymer in a good solvent) as further grafting is hindered by an entropic barrier created by the formation of the brush layer itself.[2,10] The theory for a planar brush of randomly branched polymers grafted onto the surface[44] indicates that the Gaussian

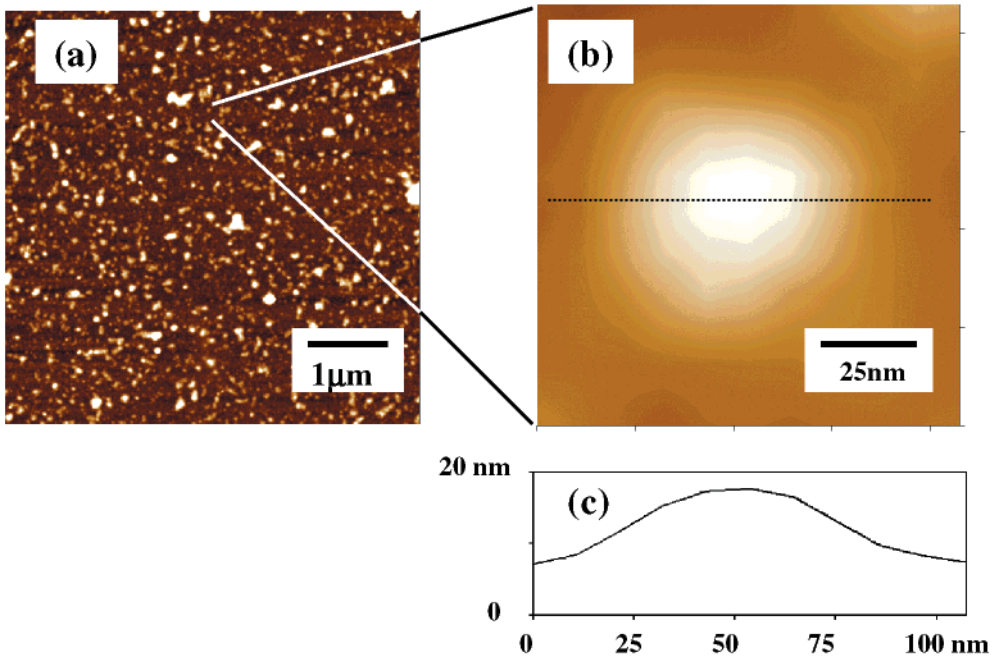

Figure 2. Tapping Mode images of grafted polymer obtained from BPEA at a ratio $[BPEA]_0:[CuBr]_0 = 125$: (a) height image, which ranges from 0 to 30 nm; (b) higher magnification image of a typical protrusion; (c) cross section taken at the position indicated by the dotted line in (b).

dimensions, R_g, of a randomly branched polymer consisting of N units scale as $R_g = a(N/\Lambda)^{1/4}$, where a is a unit size and Λ is the branching probability given as the inverse of the average number of units between two neighboring branching points. The limiting extension, $H(\Lambda)$, can be represented as $H(\Lambda) = a(N^{3/4}\Lambda^{-1/4})$. Since the degree of branching includes both branching and terminal units, which have approximately equal probability, the degree of branching equals 2Λ. If there are limiting geometric constraints on a chain grown from the surface imposed by its neighbors, the polymer may adopt a more extended conformation even if the structure is hyperbranched. Thus, the value of $H(\Lambda)$ (mean film thickness = 7.5 nm) may be larger than $2R_g$ of the hyperbranched polymers. As to R_g of branched and linear polymers, the following relation holds based on a contraction factor, $\langle R_g^2\rangle_{branched} = g\langle R_g^2\rangle_{linear}$, where the contraction factor is typically $g \approx 0.3$.[32] Because the diameter of the protrusions determined by SFM is much larger than the expected molecular dimensions given above, the protrusions must consist of more than one hyperbranched polymer chain. Protrusions with different sizes should contain different numbers of polymer chains (roughly up to 25 chains per protrusion assuming no significant geometric constraints imposed by their neighbors).

To clarify the influence of the catalyst system on the surface topography, height images of the grafted polymers obtained at different $[BPEA]_0:[CuBr]_0$ ratios are shown in Figure 3. Polymerization conditions, properties of soluble polymers, and parameters of the grafted polymers obtained are shown in Tables 1 and 2, samples 1−3. Evaluation of the areal density and of their size can also be performed by taking cross sections through the SFM height images. The size of the protrusions clearly increases with increasing ratio $[BPEA]_0:[CuBr]_0$. These observations were reproducible at different spots on the surface. The mean thickness of the polymer layers obtained from BPEA changes from 4.0 to 11.0 nm when increasing the ratio $[BPEA]_0:[CuBr]_0$ from 50 to 200 (Table 2, samples 1−3). The surface roughness increases with increasing ratio $[BPEA]_0:[CuBr]_0$, while the opposite tendency was observed for the areal density of protrusions. This means that the higher ratio may induce an increase of the size of a protrusion by accumulating the polymer chains, while a slight decrease of the number of protrusions may be due to the overlap of neighboring protrusions. The value seems to correlate slightly with the degree of branching of the ungrafted polymer. For example, sample 3 has the lowest degree of branching, suggesting that it has a higher R_g. However, since $R_g \sim DB^{-1/4}$ only, this effect cannot be large. Possibly the M_n of the grafted polymer depends on the ratio $[AB^*]_0:[catalyst]_0$. The phenomenon may occur by a process akin to crystallization of a polymer melt; that is, larger protrusions are obtained by fewer initiating sites as the lower concentration of catalyst leads to preferential growth of polymer from fewer regions of the surface. Another explanation is that the variation in the film thickness induced by the $[AB^*]_0:[catalyst]_0$ ratio is attributed to the different numbers of polymer chains attached to the surface. In this case, a higher ratio $[AB^*]_0:[catalyst]_0$ would lead to more initiating sites on the surface, due to the high solubility of catalyst in an AB* inimer. This is in agreement with the assumption described above that a protrusion consists of a certain number of hyperbranched polymer chains.

SFM measurements of the polymers obtained from BIEM were also performed (entries 7 and 8 in Tables 1 and 2). As shown in Figure 4, small protrusions are seen to be distributed over the surface, and the areal density and size of the protrusions clearly increase with increasing $[BIEM]_0:[(PPh_3)_2NiBr_2]_0$ ratio. Particularly, the polymer obtained at a ratio of 125 showed densely packed small protrusions with a relatively narrow size distribution. There was no significant difference in the surface topography between the polymers obtained from BPEA and BIEM at the $[AB^*]_0:[catalyst]_0$ ratio of 50. As can be seen in Tables 1 and 2, the mean thickness

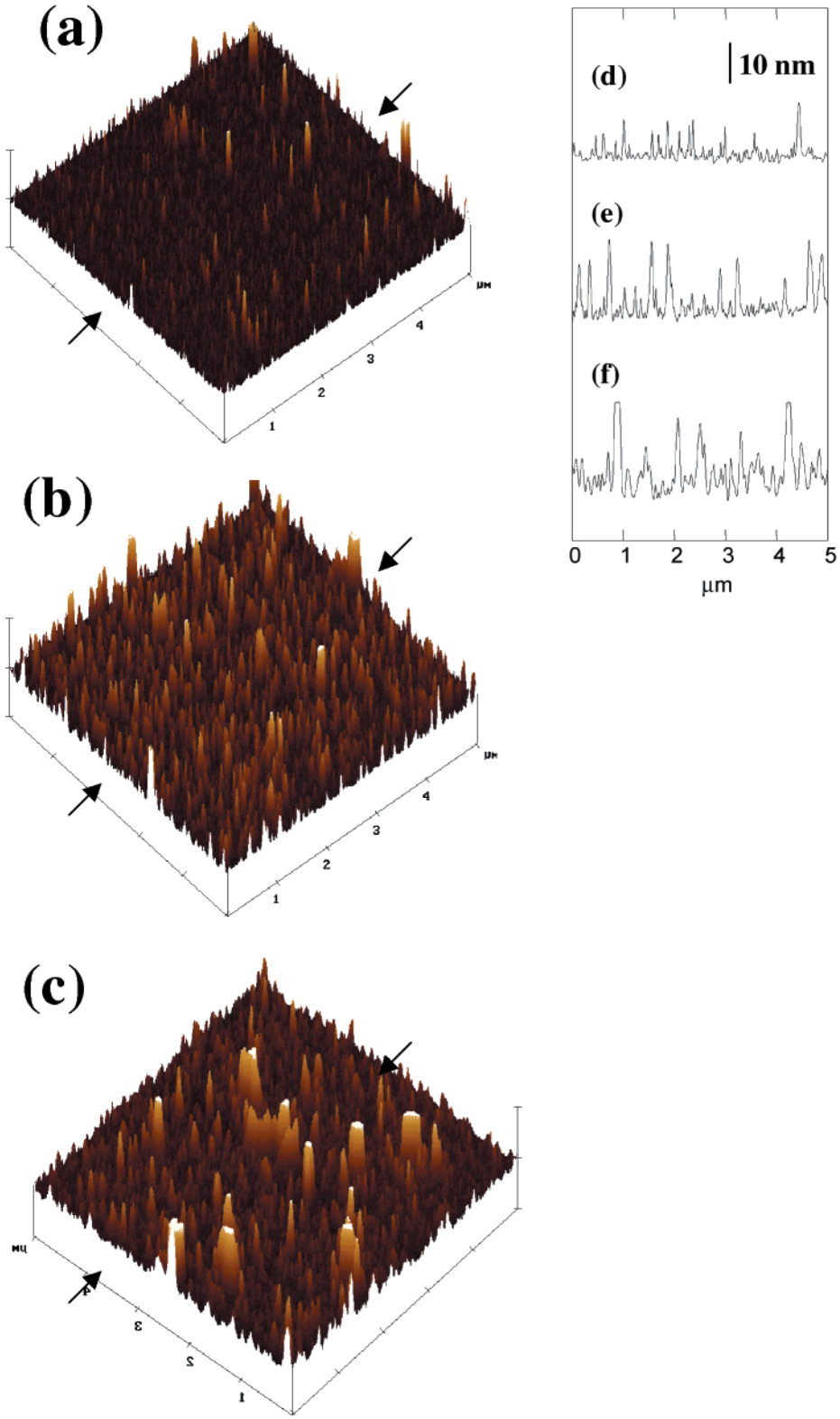

Figure 3. Three-dimensional height images of the grafted polymers obtained from BPEA at different ratios $[BPEA]_0$:$[CuBr]_0$: (a) 50; (b) 125; (c) 200. The height scale ranges from 0 to 30 nm in all height images. Cross sections through the lines indicated by the two arrows in the height images ($[BPEA]_0$:$[CuBr]_0$ ratio: (d) 50; (e) 125; (f) 200).

of the polymer layers is affected significantly by the ratio; it changes from about 4.5 nm at a ratio of 50 to about 12 nm at a ratio of 125. The dependences of the mean film thickness and the mean roughness on the $[AB^*]_0$:$[catalyst]_0$ ratio show the same tendency. These results indicate that both (meth)acrylic AB* inimers can be used to prepare surface-grafted hyperbranched polymers, and the film thickness and surface topography can be controlled by changing the $[AB^*]_0$:$[catalyst]_0$ ratio. The nanoscale polymer protrusions with different sizes and different densities, which may be due to the hyperbranched architecture, indicate that both the three-dimensional chemical structure and topological characteristics can be controlled on the surface. These

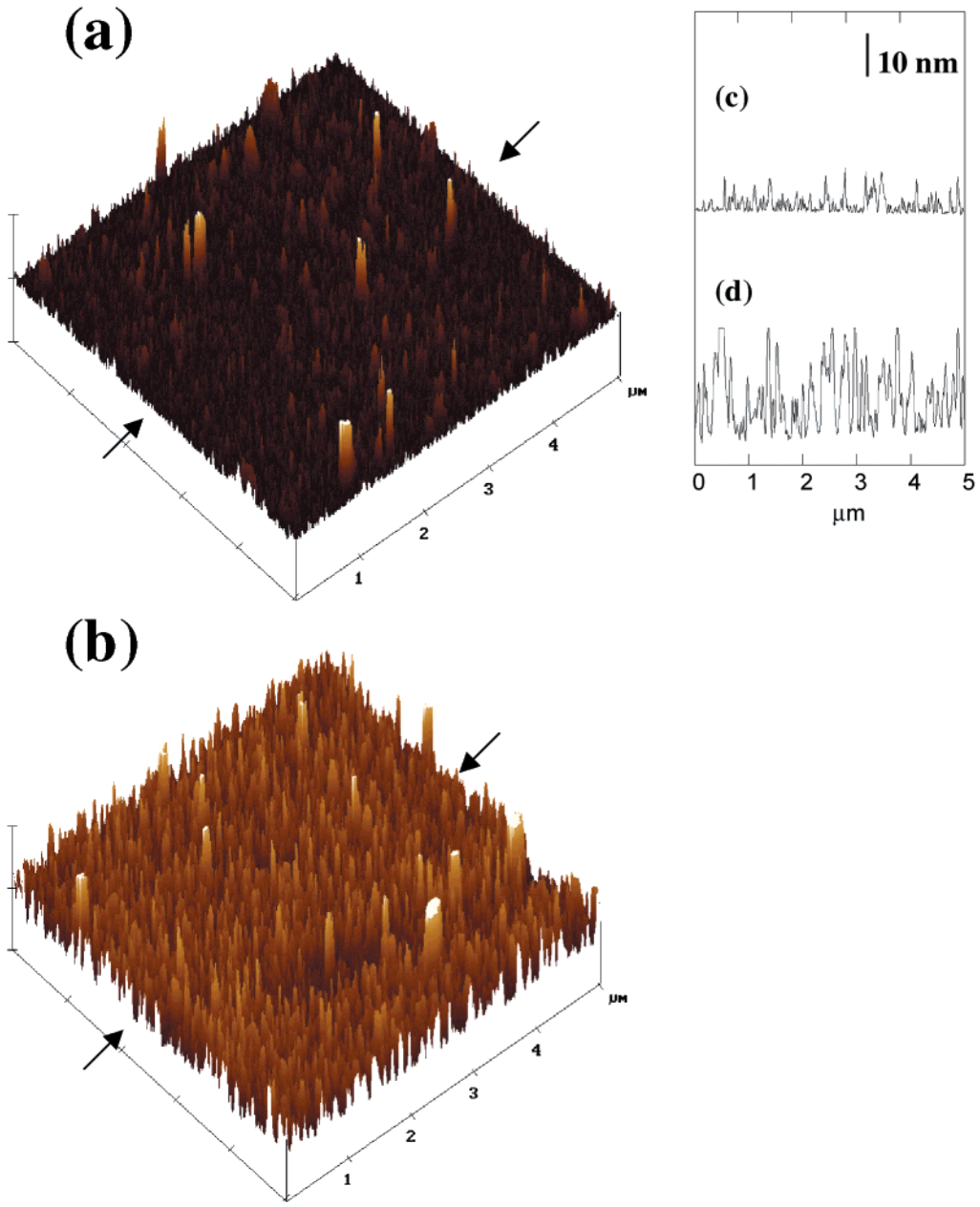

Figure 4. Three-dimensional height images of the grafted polymers obtained from BIEM at different $[BIEM]_0$:$[(PPh_3)_2NiBr_2]_0$ ratios: (a) 50; (b) 125. The height scale ranges from 0 to 30 nm in all images. Cross sections through the lines indicated by the two arrows in the height images ($[BIEM]_0$:$[(PPh_3)_2NiBr_2]_0$ ratio: (c) 50; (d) 125).

studies of SCVP of (meth)acrylic AB* inimers via ATRP with the functionalized silicon surface show that the technique is an effective tool to synthesize hyperbranched polymers from initiators attached to the surface and can provide characteristic surface topographies on the nanoscale.

Highly Branched and Linear Polymers. In the next step, we attempted to prepare surface-grafted branched and linear polymers by different polymerization procedures. Copolymerization of an AB* inimer with a conventional vinyl monomer leads to highly branched polymers, allowing for the control of the polydispersity and degree of branching.[26,34,35] For example, theoretical calculations have demonstrated that the polydispersity of polymers obtained in such a copolymerization is lower than that obtained in a homo-SCVP, and the effect of diluting the AB* inimer by a conventional monomer only decreases the degree of branching; for low comonomer ratios it can even increase.[34] A benefit of radical polymerizations over other techniques is the wide variety of monomers amenable to homo- and copolymerizations. Thus, an appropriate comonomer can be used to introduce additional functional groups. On the basis of this consideration, the copolymerization of a vinyl monomer with an AB* inimer via ATRP in the presence of the functionalized silicon wafer should be a reliable method to prepare surface-grafted branched polymers in which one can tune the architecture, physical properties, and surface topography by the choice of comonomers and their composition in the feed. For comparison, linear brushes were also prepared by surface-initiated ATRP using ethyl 2-bromo-2-isobutyrate (EBIB) as a controlling initiator.

Table 3 summarizes the characteristic features of the branched polymers obtained by copolymerization of an AB* inimer with an acrylic vinyl monomer and the linear polymer brushes. The conditions for the homo-

Table 3. Synthesis and Characterization of Highly Branched and Linear Polymers

entry	monomer	AB*	[monomer]$_0$:[AB*]$_0$:[catalyst]$_0$	M_n[a]	M_w/M_n[a]	mean film thickness[b] (nm)	mean roughness[b] (nm)	surf. coverage[c] (mg/m^2)	grafting density[d] (chains/nm^2)
9[e]	tBuA	BPEA	100:10:1	7 500	3.32	9.0	5.0	9.9	0.80
10[e,g]	tBuA		125:−:1	15 800	1.21	23	1.5	25.3	0.96
11[f]	MMA	BIEM	100:10:1	7 700	4.49	4.5	1.0	5.0	0.39
12[f,g]	MMA		125:−:1	11 600	1.25	12	2.0	13.2	0.69

[a] As determined by GPC. [b] As determined by SFM. [c] Surface coverage = film thickness × density (1.1 g/cm^3 for PMMA). [d] Grafting density = surface coverage × N_A(Avogadro's number)/M_n. [e] Bulk polymerization with CuBr/*N*,*N*′,*N*″,*N*″-pentamethyldiethylenetriamine (PMDETA) at 60 °C. [f] Bulk polymerization with $(PPh_3)_2NiBr_2$ at 100 °C. [g] Ethyl 2-bromo-2-isobutyrate (EBIB) was used as a controlling initiator (equimolar to catalyst).

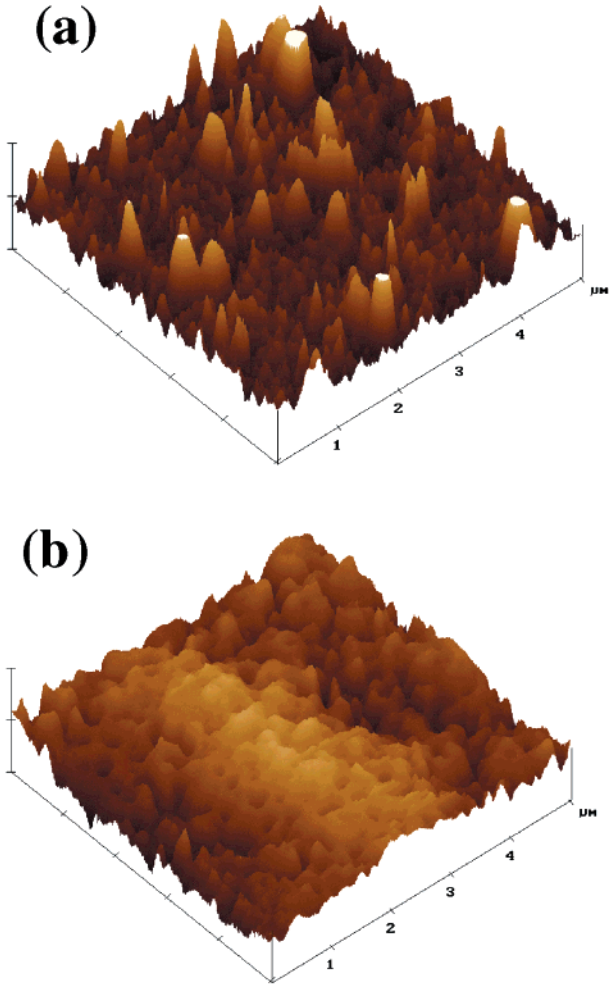

Figure 5. Three-dimensional height images of the grafted polymers obtained from (a) copolymerization of BPEA and tBuA at [tBuA]$_0$:[BPEA]$_0$:[CuBr]$_0$ ratio of 100:10:1 and (b) homopolymerization of tBuA at a ratio [tBuA]$_0$:[CuBr]$_0$ = 125. The height scale ranges from 0 to 30 nm in all images.

and copolymerizations were adjusted to yield polymers quantitatively (conversion determined by ^{1}H NMR was >90% in all cases). When BPEA was copolymerized with *tert*-butyl acrylate (tBuA) with CuBr/PMDETA at [tBuA]$_0$:[BPEA]$_0$:[CuBr]$_0$ ratio of 100:10:1, a viscous polymer with apparent M_n = 7500 and M_w/M_n = 3.32 (soluble part) was obtained. The thickness of the resulting polymer film after Soxhlet extraction, as estimated by SFM, was about 9.0 nm, which is slightly larger than that obtained by SCVP of BPEA using a similar [AB*]$_0$:[catalyst]$_0$ ratio (7.5 nm, Table 2, sample 2). SFM height images (Figure 5) depict different grafted polymers obtained from copolymerization of BPEA and tBuA (a) and from homopolymerization of tBuA (b). Large protrusions are irregularly distributed on the copolymer surface, while the polymer obtained from SCVP of BPEA shows densely packed small protrusions with a relatively narrow size distribution (Figure 3b). The value of the mean diameter of the protrusions was 50 and 30 nm, respectively.

The homopolymerization of tBuA from the functionalized silicon surface with EBIB as a controlling initiator resulted in a polymer with a low polydispersity and number-average molecular weight close to the predicted value and a polymer layer with film thickness of 23 nm. The SFM height image of this surface-grafted PtBuA revealed a relatively uniform and smooth surface with a mean roughness of about 1.5 nm in most areas. A relatively rough surface was also observed occasionally (Figure 5b). The polymer film obtained by copolymerization gave a characteristic surface topography, which is an intermediate between the polymer protrusions obtained by SCVP of BPEA and the polymer brush prepared by homopolymerization of tBuA. These results indicate that the film thickness, surface roughness, and the chemical structure of the surface-grafted polymer can be controlled by copolymerizing an AB* inimer and a conventional vinyl monomer.

The methacrylic AB* inimer, BIEM, was also copolymerized with MMA in order to obtain branched PMMA. The film was relatively thin compared to its acrylate counterpart, although there was no significant difference in the molecular weight (Table 3, entries 9 and 11). In the case of the homopolymerization of MMA, the condition was adjusted to follow the previous study of Husseman et al.,[13] in which ATRP of MMA from functionalized silicon wafers was accomplished using EBIB as a controlling initiator in the presence of $(PPh_3)_2NiBr_2$. They showed a linear relation between the molecular weight of soluble polymer and the film thickness and demonstrated that a living radical polymerization process permits the accurate control of molecular weight and polydispersity of the covalently attached polymer chains. The polymerization of tBuA was also controlled by ATRP with CuBr/PMDETA,[45] which is the same catalyst system used in this study. For these reasons, we assume that the polymer brushes obtained in this study consist of a layer of linear chains of uniform length due to the controlled character of the polymerization. If the backbone of the polymer is in an extended conformation, the film thickness of the brushes of PtBuA and PMMA should amount to the contour length $DP_n \times 0.25$ nm ≈ 30 nm. This study shows that the measured thicknesses are smaller than the calculated values, suggesting that the polymer films do not consist of fully extended chains. This is consistent with similar results of living radical polymerizations from surfaces[17] in which there were some differences between the thickness expected for fully extended chains and the

observed one, even if the measured thickness increased linearly with reaction time. The increase in the film thickness with polymerization time was also observed in a nonliving radical polymerization system,[4,5] which might give nonuniform polymer chains. Hence, chains growing from the surface should be less uniform than under homogeneous conditions, regardless of whether a "controlled" or "noncontrolled" polymerization system is used, due to the limited accessibility of the initiator and monomer in a region close to the interface and the geometric constraints resulting from the densely packed chains at the surface.

The film thickness of surface-grafted PtBuA was relatively close to the calculated limiting value, while a significant difference was found in the case of PMMA. We assume that the polymer chains obtained by homopolymerization from the surface are coiled to some extent and the degree of extension in PtBuA is higher than that in PMMA. To prove this assumption, the grafting density of these polymers was calculated by assuming a mass density of 1.1 g/cm^3 in all cases. The value observed in the polymer prepared by homopolymerization of MMA was approximately 0.7 chains/nm^2, which is close to the value reported by Yamamoto et al.[46,47] The authors prepared PMMA brushes by Cu-based ATRP from a silicon surface functionalized with 2-(4-chlorosulfonylphenyl)ethyltrimethoxysilane. The polymer film obtained from copolymerization of BIEM and MMA had a lower areal density of chains. On the other hand, the values of the acrylate counterparts were about 0.9 chains/nm^2. The difference in the average area occupied by each polymer chain between the brushes obtained from tBuA and MMA may be due to the different geometric constraints, depending upon the size of the monomer, the flexibility of the polymer main chain, and/or different grafting efficiencies, namely different numbers of potential initiators per one polymer chain.

Surface Composition. XPS was used to determine the surface composition of the hyperbranched polymers obtained by SCVP from the functionalized silicon wafer. Figure 6a shows a survey scan spectrum of the polymer layer prepared from BPEA, which detect three elements: oxygen (533 eV), carbon (285 eV), and silicon (150 and 98 eV). Further, bromine peaks assigned to Br_{3d} (70 eV), $Br_{3p3/2}$ (184 eV), $Br_{3p1/2}$ (191 eV), and Br_{3s} (278 eV) are visible. The increase in the intensity of the carbon signal relative to the silicon and oxygen, compared to the functionalized silicon wafer as shown in Figure 1, indicates the addition of the polymer to the surface. There are still silicon peaks, suggesting that the thickness of the polymer layer is smaller than the photoelectron escape depth. These results are consistent with the thickness and surface topography of the polymer layer observed by SFM. The initial intensity of the Br peaks decreased during the time required to obtain a distinguishable survey spectrum with high S/N ratio, which was also observed for the functionalized silicon wafer. The relative atomic composition estimated from the corrected Br peak was 13% Br and 87% C, which agrees with the expected value based on the chemical composition of BPEA (11% Br). Here, the degree of branching may induce a higher surface enrichment of bromine groups, because a bromine atom acting as a branching point migrates to an end group of the branched chain formed by the next monomer addition, and repetition of this step would bring a bromine atom to the outer surface, as illustrated in Scheme 1. On the other hand, such surface enrichment may not occur in the case of a linear poly(BPEA), where an inactivated bromine atom in BPEA still exists along the main chain.

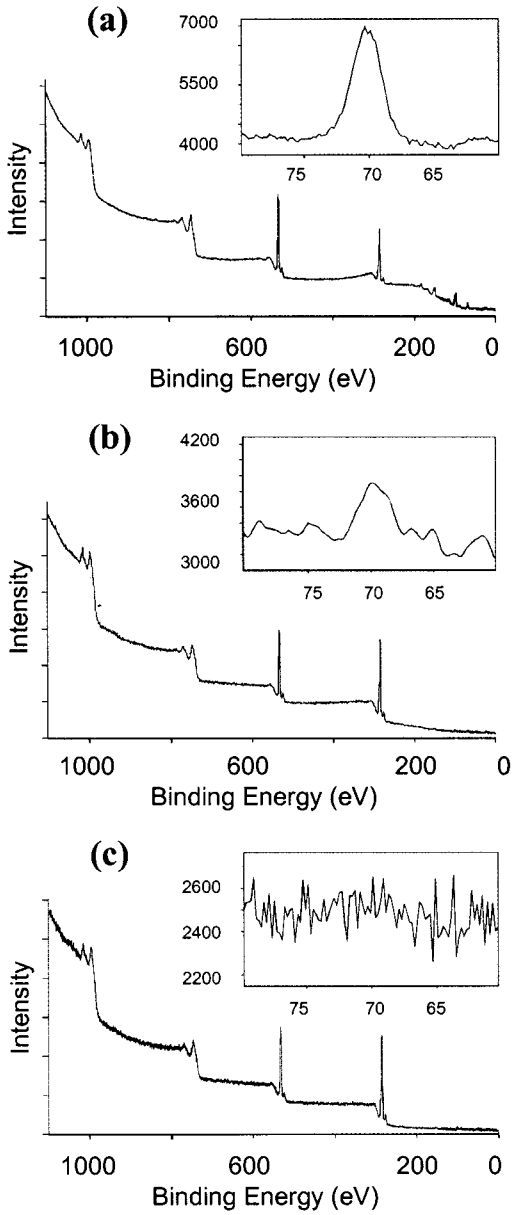

Figure 6. XPS survey spectra of the grafted polymers obtained from (a) SCVP of BPEA at a ratio $[BPEA]_0$:$[CuBr]_0$ = 125, (b) copolymerization of BPEA and tBuA at $[tBuA]_0$:$[BPEA]_0$:$[CuBr]_0$ ratio of 100:10:1, and (c) homopolymerization of tBuA at a ratio $[tBuA]_0$:$[CuBr]_0$ = 125. Insets: region associated with the peak derived from bromine.

To clarify the correlation of the intensity of the bromine peaks and the three-dimensional structure of the polymer layer grafted from the surface, XPS measurements were also carried out for a linear polymer brush prepared by a surface-initiated ATRP of a conventional vinyl monomer (tBuA) and a branched polymer obtained by copolymerization of BPEA and tBuA. The XPS spectra of these polymer layers exhibit only C and O peaks, as can be seen in Figure 6b,c, indicating that the samples are free from catalyst residues. Hardly any silicon signal was observed, showing that the silicon substrates were covered completely with a polymer layer and the thickness of the layer was larger than the

escape depth of the photoelectrons (about 11 nm[48]). The atomic composition (77% C and 23% O) of the linear polymer brush agreed well with the calculated value (22% O), indicating that a PtBuA layer formed on the surface. However, no bromine peak was detected, as can be seen in Figure 6c. The bromine peak was clearly visible on the surface of the functionalized silicon wafer prior to the polymerization. This is in accord with similar XPS results reported by Matyjaszewski et al.[17] in which the bromine signal was reduced by 50% during a surface-initiated ATRP of styrene. They have also demonstrated that the bromine could be either lost through some termination/elimination/transfer event or still be present at the termini of the majority of the chains which are, however, not readily detectable by the XPS technique because the chains are not fully extended. The nonuniformity of chain ends should lead to a broader distribution of bromine atoms and a less intense XPS signal. Recently, Bednarek et al. also reported that bromine-terminated polymers prepared by ATRP were gradually converted into inactive macromolecules devoid of terminal bromine in the course of polymerization of acrylate monomers with CuBr/PMDETA.[49] The relative atomic composition of carbon and oxygen in the polymer obtained by the copolymerization was almost the same as the one in the linear polymer brush, but a small signal remained for the bromine at 70 eV (approximately 1% Br), as can be seen in Figure 6b. Obviously, the reduction of the bromine signal detected on the copolymer surface is due to dilution of the active centers by tBuA unit. It was anticipated that the number of Br atoms per monomer unit is unity for the polymer obtained from SCVP, whereas it is 1/(comonomer ratio in the feed) for the copolymer and 1/(degree of polymerization) for PtBuA. In other words, the Br signal for SCVP should clearly be the largest, in agreement with the XPS measurements. Hence, the strong intensity of the bromine signal in the hyperbranched polymer obtained by SCVP relative to that in the linear and branched polymers demonstrates that the functional bromine end groups exist predominantly on the surface, and their number is much larger compared to linear polymers. Therefore, these polymer films are attractive candidates for the preparation of surfaces with high functionalities.

Conclusions

We present the first report of surface-initiated SCVP of (meth)acrylic AB* inimers using a silicon wafer functionalized with monolayers of initiators for controlled/"living" radical polymerization. Self-condensing ATRP of the initiator-monomer, BPEA, yields polymer films with a high degree of branching and with a characteristic surface topography. The size and density of the nanoscale protrusions obtained on the surface and the film thickness depend on the polymerization conditions, such as the ratio $[BPEA]_0$:$[catalyst]_0$. Similar results were obtained by SCVP of BIEM. In this way, we have been able to create novel surface architectures, in which the characteristic nanoprotrusions with different densities and sizes are composed of hyperbranched polymers tethered directly to the surface. The differences in the surface topography and film thickness between the polymer protrusions obtained from SCVP of an AB* inimer, the polymer brushes obtained by ATRP of a conventional monomer, and the intermediate structures prepared by copolymerization of an AB* inimer and a conventional vinyl monomer were also confirmed by SFM. The chain architecture and chemical structure can be modified by copolymerization of AB* monomers with conventional vinyl monomers leading to a facile, one-pot synthesis of surface-grafted branched polymers. The difference in the Br content at the surfaces of hyperbranched, branched, and linear polymers was confirmed by XPS, suggesting the feasibility to control the surface chemical functionality. Thus, a well-controlled synthesis for the materials is considered to lead to the creation of novel materials that are controllable on a nanoscopic scale and have a chemically sensitive interface. The principal result of the work reported herein is a demonstration of the utility of surface-initiated SCVP via ATRP to prepare surface-grafted hyperbranched and branched polymers having characteristic architecture and topography. After suitable modification of end groups and/or linear segments, these polymers should have interesting properties for many applications, such as sensors, bioadhesives, etc.

Acknowledgment. The authors thank G. Sauer for the XPS measurements. H.M. acknowledges an Overseas Research Fellowship by the Ministry of Education, Science, Sports, and Culture of Japan and Prof. Minoru Terano (Japan Advanced Institute of Science and Technology) for substantial support. A.B. thanks Stiftung Stipendien-Fonds des Verbandes der Chemischen Industrie and BMBF for a Kekulé fellowship. A.H.E.M and G.K. acknowledge support through the Deutsche Forschungsgemeinschaft (Schwerpunkt " Benetzung und Strukturbildung an Grenzflächen").

References and Notes

(1) Zhao, B.; Brittain, W. J. *Prog. Polym. Sci.* **2000**, *25*, 677.
(2) Luzinov, I.; Julthongpiput, D.; Malz, H.; Pionteck, J.; Tsukruk, V. V. *Macromolecules* **2000**, *33*, 1043.
(3) (a) Dan, N.; Tirrell, M. *Macromolecules* **1993**, *26*, 4310. (b) Belder, G. F.; ten Brinke, G.; Hadziioannou, G. *Langmuir* **1997**, *13*, 4102. (c) Mansky, P.; Liu, Y.; Huang, E.; Russell, T. P.; Hawker, C. J. *Science* **1997**, *275*, 1458. (d) Jordan, R.; Graf, K.; Riegler, H.; Unger, K. K. *J. Chem. Soc., Chem. Commun.* **1996**, *9*, 1025. (e) Hadziioannou, G.; Patel, S.; Granick, S.; Tirrell, M. *J. Am. Chem. Soc.* **1986**, *108*, 2869.
(4) Prucker, O.; Rühe, J. *Langmuir* **1998**, *14*, 6893.
(5) Biesalski, M.; Rühe, J. *Macromolecules* **1999**, *32*, 2309.
(6) (a) Prucker, O.; Rühe, J. *Macromolecules* **1998**, *31*, 592. (b) Prucker, O.; Rühe, J. *Macromolecules* **1998**, *31*, 602.
(7) (a) Israels, R.; Gersappe, D.; Fasolka, M.; Roberts, V. A.; Balazs, A. C. *Macromolecules* **1994**, *27*, 6679. (b) Sevick, E. M.; Williams, D. R. M. *Macromolecules* **1994**, *27*, 5285. (c) Pincus, P. *Macromolecules* **1991**, *24*, 2912. (d) Takei, Y. G.; Aoki, T.; Sanui, K.; Ogata, N.; Sakurai, Y.; Okano, T. *Macromolecules* **1994**, *27*, 6163. (e) Liu, Y.; Quinn, J.; Rafailovich, M. H.; Sokolov, J.; Zhong, X.; Eisenberg, A. *Macromolecules* **1995**, *28*, 6347.
(8) Zhao, B.; Brittain, W. J. *Macromolecules* **2000**, *33*, 342.
(9) Jordan, R.; Ulman, A. *J. Am. Chem. Soc.* **1998**, *120*, 243.
(10) Jordan, R.; Ulman, A.; Kang, J. F.; Rafailovich, M. H.; Sokolov, J. *J. Am. Chem. Soc.* **1999**, *121*, 1016.
(11) Ingall, M. D. K.; Honeyman, C. H.; Mercure, J. V.; Bianconi, P. A.; Kunz, R. R. *J. Am. Chem. Soc.* **1999**, *121*, 3607.
(12) Ejaz, M.; Yamamoto, S.; Ohno, K.; Tsujii, Y.; Fukuda, T. *Macromolecules* **1998**, *31*, 5934.
(13) Husseman, M.; Malmström, E. E.; McNamara, M.; Mate, M.; Mecerreyes, D.; Benoit, D. G.; Hedrick, J. L.; Mansky, P.; Huang, E.; Russell, T. P.; Hawker, C. J. *Macromolecules* **1999**, *32*, 1424.
(14) Huang, X.; Wirth, M. J. *Macromolecules* **1999**, *32*, 1694.
(15) Huang, X.; Doneski, L. J.; Wirth, M. J. *Anal. Chem.* **1998**, *70*, 4023.
(16) de Boer, B.; Simon, H. K.; Werts, M. P. L.; van der Vegte, E. W.; Hadziioannou, G. *Macromolecules* **2000**, *33*, 349.
(17) Matyjaszewski, K.; Miller, P. J.; Shukla, N.; Immaraporn, B.; Gelman, A.; Luokala, B. B.; Siclovan, T. M.; Kickelbick,

G.; Vallant, T.; Hoffmann, H.; Pakula, T. *Macromolecules* **1999**, *32*, 8716.
(18) Kin, N. Y.; Jeon, N. L.; Choi, I. S.; Takami, S.; Harada, Y.; Finnie, K. R.; Girolami, G. S.; Nuzzo, R. G.; Whitesides, G. M.; Laibinis, P. E. *Macromolecules* **2000**, *33*, 2793.
(19) Weck, M.; Jackiw, J. J.; Rossi, R. R.; Weiss, P. S.; Grubbs, R. H. *J. Am. Chem. Soc.* **1999**, *121*, 4088.
(20) Husemann, M.; Mecerreyes, D.; Hawker, C. J.; Hedrick, J. L.; Shah, R.; Abbott, N. L. *Angew. Chem., Int. Ed. Engl.* **1999**, *38*, 647.
(21) (a) Tully, D. C.; Trimble, A. R.; Fréchet, J. M. J.; Wilder, K.; Quate, C. F. *Chem. Mater.* **1999**, *11*, 2892. (b) Tully, D. C.; Wilder, K.; Fréchet, J. M. J.; Trimble, A. R.; Quate, C. F. *Adv. Mater.* **1999**, *11*, 314. (c) Li, J.; Piehler, L. T.: Qin, D.; Baker, J. R.; Tomalia, D. A. *Langmuir* **2000**, *16*, 5613. (d) Hierlemann, A.; Campbell, J. K.; Baker, L. A.; Crooks, R. M.; Ricco, A. J. *J. Am. Chem. Soc.* **1998**, *120*, 5323.
(22) Zhou, Y.; Bruening, M. L.; Bergbreiter, D. E.; Crooks, R. M.; Wells, M. *J. Am. Chem. Soc.* **1996**, *118*, 3773.
(23) (a) Bruening, M. L.; Zhou, Y.; Aguilar, G.; Agee, R.; Bergbreiter, D. E.; Crooks, R. M. *Langmuir* **1997**, *13*, 770. (b) Peez, R. F.; Dermody, D. L.; Franchina, J. G.; Jones, S. J.; Bruening, M. L.; Bergbreiter, D. E.; Crooks, R. M. *Langmuir* **1998**, *14*, 4232. (c) Ghosh, P.; Amirpour, M. L.; Lackowski, W. M.; Pishko, M. V.; Crooks, R. M. *Angew. Chem., Int. Ed.* **1999**, *38*, 1592. (d) Lackowski, W. M.; Ghosh, P.; Crooks, R. M. *J. Am. Chem. Soc.* **1999**, *121*, 1419. (e) Ghosh, P.; Lackowski, W. M.; Crooks, R. M. *Macromolecules* **2001**, *34*, 1230. (f) Franchina, J. G.; Lackowski, W. M.; Dermody, D. L.; Crooks, R. M.; Bergbreiter, D. E.; Sirkar, K.; Russell, R. J.; Pishko, M. V. *Anal. Chem.* **1999**, *71*, 3133. (g) Zhou, M.; Bruening, M. L.; Zhou, Y.; Bergbreiter, D. E.; Crooks, R. M. *Isr. J. Chem.* **1997**, *37*, 277. (h) Aoki, A.; Ghosh, P.; Crooks, R. M. *Langmuir* **1999**, *15*, 7418.
(24) (a) Fréchet, J. M. J.; Henmi, M.; Gitsov, I.; Aoshima, S.; Leduc, M. R.; Grubbs, R. B. *Science* **1995**, *269*, 1080.
(25) Hawker, C. J.; Fréchet, J. M. J.; Grubbs, R. B.; Dao, J. *J. Am. Chem. Soc.* **1995**, *117*, 10763.
(26) Gaynor, S. G.; Edelman, S.; Matyjaszewski, K. *Macromolecules* **1996**, *29*, 1079.
(27) Matyjaszewski, K.; Gaynor, S. G.; Kulfan, A.; Podwika, M. *Macromolecules* **1997**, *30*, 5192.
(28) Matyjaszewski, K.; Gaynor, S. G.; Müller, A. H. E. *Macromolecules* **1997**, *30*, 7034.
(29) Matyjaszewski, K.; Gaynor, S. G. *Macromolecules* **1997**, *30*, 7042.
(30) Cheng, G.; Simon, P. F. W.; Hartenstein, M.; Müller, A. H. E. *Macromol. Rapid Commun.* **2000**, *21*, 846.
(31) Weimer, M. W.; Fréchet, J. M. J.; Gitsov. I. *J. Polym. Sci., Part A: Polym. Chem.* **1998**, *36*, 955.
(32) Simon, P. F. W.; Radke, W.; Müller, A. H. E. *Macromol. Rapid Commun.* **1997**, *18*, 865.
(33) Sunder, A.; Hanselmann, R.; Frey, H.; Mülhaupt, R. *Macromolecules* **1999**, *32*, 4240.
(34) Litvinenko, G. I.; Simon, P. F. W.; Müller, A. H. E. *Macromolecules* **1999**, *32*, 2410.
(35) Simon, P. F. W.; Müller, A. H. E. *Macromolecules* **2001**, in press.
(36) Yan, D.; Müller, A. H. E.; Matyjaszewski, K. *Macromolecules* **1997**, *30*, 7024.
(37) We note that there still is controversy on the scratch test: See: Thomas, R. C.; Houston, J. E.; Michalske, T. A.; Crooks, R. M. *Science* **1993**, *259*, 1883. However, we are able to quantitatively control the tip indentation (Knoll, A.; Magerle, R.; Krausch, G. *Macromolecules* **2001**, *34*, 4159), thereby improving the reliability of the procedure.
(38) Wasserman, S. R.; Tao, Y.; Whitesides, G. M. *Langmuir* **1989**, *5*, 1074.
(39) Shah, R. R.; Merreceyes, D.; Husemann, M.; Rees, I.; Abbott, N. L.; Hawker, C. J.; Hedrick, J. L. *Macromolecules* **2000**, *33*, 597.
(40) Radke, W.; Litvinenko, G.; Müller, A. H. E. *Macromolecules* **1998**, *31*, 239.
(41) Yan, D.; Zhou, Z.; Müller, A. H. E. *Macromolecules* **1999**, *32*, 245.
(42) Müller, A. H. E.; Yan, D.; Wulkow, M. *Macromolecules* **1997**, *30*, 7015.
(43) The following control experiment was carried out: the silicon wafer was treated in the THF solution of hyperbranched polymer of BPEA formed in solution, followed by Soxhlet extraction in THF for 24 h. No adsorbed polymer was observed by SFM, indicating that the polymer adsorbed could be removed by washing.
(44) Zhulina, E. B.; Vilgis, T. A. *Macromolecules* **1995**, *28*, 1008.
(45) Davis, K. A.; Matyjaszewski, K. *Macromolecules* **2000**, *33*, 4039.
(46) Yamamoto, S.; Ejaz, M.; Tsujii, Y.; Matsumoto, M.; Fukuda, T. *Macromolecules* **2000**, *33*, 5602.
(47) Yamamoto, S.; Ejaz, M.; Tsujii, Y.; Fukuda, T. *Macromolecules* **2000**, *33*, 5608.
(48) (a) Seah, M. P.; Dench, W. A. *Surf. Interface. Anal.* **1979**, *1*, 2. (b) Chen, X.; Gardella, J. A., Jr.; Kumler, P. L. *Macromolecules* **1993**, *26*, 3778.
(49) Bednarek, M.; Biedron, T.; Kubisa, P. *Macromol. Chem. Phys.* **2000**, *201*, 58.

MA0019048